Received: 6 April 2024 | Revised: 25 July 2024 | Accepted: 29 August 2024

DOI: 10.1111/ejn.16543

RESEARCH REPORT

EJN European Journal of Neuroscience FENS WILEY

Progression of hippocampal subfield atrophy and asymmetry in Alzheimer's disease

Jingjing Xu | Sijia Tan | Jiaqi Wen | Minming Zhang | For the Alzheimer's Disease Neuroimaging Initiative | Xiaojun Xu

Department of Radiology, The Second Affiliated Hospital, Zhejiang University School of Medicine. No.88 Jiefang Road, Hangzhou, China

Correspondence
Xiaojun Xu, Department of Radiology, The Second Affiliated Hospital, Zhejiang University School of Medicine. No.88 Jiefang Road, Shangcheng District, Hangzhou, China, 310009.
Email: xxjmailbox@zju.edu.cn

Funding information
This work was supported by the National Natural Science Foundation of China (Grant No. 82202089 82371906). Data collection and sharing for this project were funded by the Alzheimer's Disease Neuroimaging Initiative (ADNI) (National Institutes of Health Grant U01 AG024904) and DOD ADNI (Department of Defense award number W81XWH-12-2-0012). ADNI was funded by the National Institute on Aging, the National Institute of Biomedical Imaging and Bioengineering, and through generous contributions from the following: AbbVie, Alzheimer's Association; Alzheimer's Drug Discovery Foundation; Araclon Biotech; BioClinica, Inc.; Biogen; Bristol-Myers Squibb Company; CereSpir, Inc.; Cogstate; Eisai Inc.; Elan Pharmaceuticals, Inc.; Eli Lilly and

Abstract

Alzheimer's disease (AD) affects the hippocampus during its progression, but the specific observable changes of hippocampal subfields during disease progression remain poorly understood. In this study, we employed an event-based model (EBM) to determine the sequence of occurrence of hippocampal subfield atrophy in mild cognitive impairment (MCI) and AD cohorts. Subjects (207) were included: 86 MCI, 53 AD, and 68 healthy controls from the Alzheimer's Disease Neuroimaging Initiative (ADNI). Participants underwent structural magnetic resonance imaging (MRI) scans to analyse the hippocampal subfields. We assigned each patient to a specific EBM stage, based on the number of their abnormal subfields. A combination of 2-year follow-up MRI scans were applied to demonstrate the longitudinal consistency and utility of the model's staging system. The model estimated that the earliest atrophy occurs in the hippocampal fissure, then spreading to other subregions in both MCI and AD. We identified a marked divergence between the sequences of left and right hippocampal subfields atrophy, so inter-hemispheric asymmetry pattern was further analysed. The sequence of asymmetry index (AI) increases beginning in the molecular and granule cell layers of the dentate gyrus (GC-ML-DG), cornus ammonis (CA) 4, and the molecular layer (ML). Longitudinal analysis confirms the efficacy of the model. In addition, the model stages were significantly correlated with patients' memory scores ($p < .05$). Collectively,

Abbreviations: AD, Alzheimer's disease; ADAS-Cog, Alzheimer's disease assessment schedule - cognition; ADNI, Alzheimer's Disease Neuroimaging Initiative; AI, asymmetry index; ANOVA, analysis of variance; BC, Bhattacharrya coefficient; CA, cornus ammonis; CDR, Clinical Dementia Rating; DG, dentate gyrus; EBM, event-based model; eHP, entire hippocampus; F, female; GC-ML-DG, granule cell layers of the dentate gyrus; HATA, hippocampal amygdala transition area; HP, hippocampus; M, male; MCI, mild cognitive impairment; ML, molecular layer; MMSE, Mini-Mental State Examination; NC, normal control; PET, positron emission tomography; RAVLT, Rey Auditory Verbal Learning Test; SD, standard deviations; VR, volume ratio; WMS-R, Wechsler Memory Scale.

Data used in preparation of this article were obtained from the Alzheimer's Disease Neuroimaging Initiative (ADNI) database (adni.loni.usc.edu). As such, the investigators within the ADNI contributed to the design and implementation of ADNI and/or provided data but did not participate in analysis or writing of this report. A complete listing of ADNI investigators can be found at: http://adni.loni.usc.edu/wp-content/uploads/how_to_apply/ADNI_Acknowledgement_List.pdf.

Company; EuroImmun; F. Hoffmann-La Roche Ltd. and its affiliated company Genentech, Inc.; Fujirebio; GE Healthcare; IXICO Ltd.; Janssen Alzheimer's Immunotherapy Research & Development, LLC.; Johnson & Johnson Pharmaceutical Research & Development LLC.; Lumosity; Lundbeck; Merck & Co., Inc.; Meso Scale Diagnostics, LLC.; NeuroRx Research; Neurotrack Technologies; Novartis Pharmaceuticals Corporation; Pfizer Inc.; Piramal Imaging; Servier; Takeda Pharmaceutical Company; and Transition Therapeutics. The Canadian Institutes of Health Research is providing funds to support ADNI clinical sites in Canada. Private sector contributions are facilitated by the Foundation for the National Institutes of Health (www.fnih.org). The grantee organization is the Northern California Institute for Research and Education, and the study is coordinated by the Alzheimer's Therapeutic Research Institute at the University of Southern California. ADNI data are disseminated by the Laboratory for Neuro Imaging at the University of Southern California.

Edited by: Yan Zhang

we used a data-driven method to provide new insight into AD hippocampal progression. The present model could aid in understanding of the disease stages, as well as tracking memory decline.

KEYWORDS

Alzheimer's disease, disease progression, event-based model, hippocampus

1 | INTRODUCTION

Based on neuropathological data, the hippocampal subfields show differential volumetric changes during Alzheimer's disease (AD) progression (Braak & Braak, 1991; Fukutani et al., 2000; Lace et al., 2009; Schönheit et al., 2004). Neuroimaging researchers have captured corresponding morphological changes within the hippocampus (HP; Apostolova et al., 2010; de Flores et al., 2015; Pluta et al., 2012). For example, most magnetic resonance imaging (MRI) volumetric studies highlighted a focal atrophy in the Cornu Ammonis 1 (CA1) in AD and mild cognitive impairment (MCI) patients (Boutet et al., 2014; Mueller & Weiner, 2009; Tang et al., 2015; Wisse et al., 2014). In a few studies, early volume losses were also revealed in the subiculum (de Flores et al., 2015), in the CA4/the dentate gyrus (DG) (Pluta et al., 2012), and in the CA3/DG (Yassa et al., 2010). The CA1 focal atrophy pattern was even more pronounced in MCI patients who later progressed to AD compared with those stable MCIs (Apostolova, Mosconi, et al., 2010). A recent study found the progression from MCI to AD involved a more restricted number of hippocampal subfields (Punzi et al., 2024). These reports stress the importance of MRI-based hippocampal subfield measurements as sensitive markers of AD processes and emphasize selective subfield atrophy pattern which correlated with different clinical stages of AD.

Memory loss is often the first and most prominent symptom of AD. The HP plays an important role in memory (Eichenbaum, 2004). However, the hippocampal subfields are differently involved in memory impairment, because each of which has distinct neurological functions (O'Mara & Aggleton, 2019). Volumetric analysis on healthy aging, MCI, and AD showed that CA1 and subiculum have important roles in visual and verbal episodic memory (Zeng et al., 2021; Zhao et al., 2019). Other studies suggested that DG and CA3 may be more central to encoding and retrieval processes than other subfields (Zheng et al., 2018). It explained why some studies have not found an association between whole hippocampal volume and memory performances in AD (Clark et al., 2020). Based on these findings, subfield atrophy may account for memory dysfunction in the different stages of AD. However, studies about the role of hippocampal subfields for memory of patients with AD progression are not well characterized.

Recent research has linked asymmetric alterations of hippocampal subfields to MCI and AD progression (Huang et al., 2020; Parker et al., 2019; Sarica et al., 2018; Zhao et al., 2019). Some researchers found rightward lateralization of hippocampal subfields in MCI, while leftward lateralization was evident in AD patients (Liu et al., 2018; Roe et al., 2021; Weise et al., 2018; Wu et al., 2020). Jahanshahi et al. used the asymmetry index (AI) to investigate the subfields laterality and found significantly difference of AI between AD and MCI, as well as between AD and normal control (in subfields such as molecular layer (ML), GC-ML-DG, and CA4) (Jahanshahi et al., 2023). A general trend of increased degree of asymmetry with increasing severity of diagnosis was observed in MCI and AD groups.

Overall, evidence suggests that hippocampal subfields atrophy and asymmetry changes were in a non-random manner during disease progression and memory impairment in the course of AD. However, it is unknown whether there is a consistent and identifiable order in which structural changes progress affecting different hippocampal subfields over time. Additionally, previous findings have been mainly confirmed by cross-section comparisons between healthy aging, MCI, and AD groups. Little attention has been given to longitudinal analysis in AD disease continuum. In the present study, we construct an event-based model (EBM) (Fonteijn et al., 2012) to simulate AD disease progression and to investigate the progression of hippocampal subfields atrophy and asymmetry changes. Therefore, we hypothesized that (1) there is a sequence in which subfields become atrophic and asymmetric; (2) this sequence is similar in both MCI and AD patients.

2 | MATERIALS AND METHODS

2.1 | Subjects

Subjects were from the ADNI database downloaded from the website (adni.loni.usc.edu). Inclusive and exclusive criteria are at http://www.adni-info.org. The ADNI criteria for normal controls (NC) were (1) no complain for cognition decline, (2) a Mini-Mental State Examination (MMSE) score of at least 24, and (3) a Clinical Dementia Rating (CDR) score of 0. The ADNI criteria for MCI were (1) a complain of subjective memory decline, (2) objective memory decrease using the Wechsler Memory Scale (WMS-R) logical memory test (Wechsler, 1987), (3) an MMSE score ≥ 24, (4) a CDR score of .5, and (5) a diagnosis of dementia could not be made at the time of screening by the site physician. The ADNI criteria for AD were (1) an MMSE scores between 20 and 26 and (2) a CDR of .5 or 1.0 at baseline (Petersen et al., 2010).

Based on the above criteria, we identified 207 subjects from ADNI-2, including 68 NC, 86 MCI, and 53 AD. Subjects who had a non-accelerated T1 MRI screening scan at baseline and 2-year follow-up, and memory score at baseline were included for our study. Written informed consent was obtained from all participants or their authorized representatives. Subjects who underwent a scanning session but displayed incomplete clinical and demographic information and/or explained technical issues in their MRI raw data (severe motion, missing volumes, or corrupted files) were excluded from the study sample (Supplementary Figure. S1).

2.2 | Structural magnetic resonance imaging

The ADNI-2 non-accelerated sagittal 3D T1-weighted MRI sequence (repetition time = 7.34 ms, echo time = 3.04 ms, inversion time = 400 ms, flip angle = 11°, matrix size = 256 × 256, voxel size (VS) = 1 × 1 × 1.2 mm, field of view (FOV) = 260, 196 slices) was performed for each participant for the baseline and the follow-up data. The ADNI-2 sequence was chosen as it has previously been used in several large-scale longitudinal studies of neurodegenerative and mental health disorders (Hedges et al., 2022; Tognin et al., 2020).

2.3 | Hippocampal subfields volume estimation

Volumetric measures of hippocampal subfields were performed using FreeSurfer (version 6.0) (http://surfer.nmr.mgh.harvard.edu). For each subject, we used the FreeSurfer cross-sectional and longitudinal streams. The baseline and follow-up scans are processed independently for each subject. For longitudinal analysis, FreeSurfer uses results from the cross-sectional analysis to create an unbiased within-subject template; both of which are then used to initialise the final longitudinal processing stage (https://surfer.nmr.mgh.harvard.edu/fswiki/LongitudinalProcessing).

Automated segmentation of the hippocampal subfields was performed based on a computational atlas of the hippocampal formation using a combination of ex vivo and in vivo MRI data (Iglesias et al., 2015). The atlas includes the hippocampal tail, subiculum, CA1, CA3, CA4 (do not include the proximal section of CA3), the hippocampal fissure, presubiculum, parasubiculum, the molecular layer (ML), the molecular and granule cell layers of the dentate gyrus (GC-ML-DG), fimbria, and the hippocampal amygdala transition area (HATA). It is important to consider the relationship of the bilateral hippocampal subfields and the entire HP (eHP), which varies between individuals (Burwell & Agster, 2008; Xu et al., 2022). In this study, we used subfield-to-eHP volume ratio (VR) for further statistical analyses. The formula was:

$$\mathrm{VR} = \frac{(\mathrm{Left} + \mathrm{Right})}{(\mathrm{Left} + \mathrm{Right})} * 100$$

We also calculated left subfield-to-eHP VR and right subfield-to-eHP VR for statistical analyses.

2.4 | Hippocampal subfields AI

As previously studied (Eshaghi et al., 2018; Fonteijn et al., 2011; Young et al., 2014), we calculated the volumetric AI by the following formula:

$$\mathrm{AI} = \frac{|\mathrm{Left} - \mathrm{Right}|}{|\mathrm{Left} + \mathrm{Right}|} * 100$$

2.5 | The EBM

We used the EBM, as previously studied (Eshaghi et al., 2018; Fonteijn et al., 2011; Young et al., 2014), to estimate the maximum-likelihood sequence in which hippocampal subfields become atrophic and asymmetric over time based on our NC and MCI/AD patients. We normalized all measures using a linear model: $\mathrm{measure}_{ad} = \frac{|\mathrm{measure} - \mathrm{average}_{NC}|}{1.5 * \mathrm{SD}_{NC}}$. Standard deviations (SD; ±1.5) from the means of the NC were defined as an abnormal event for each biomarker of an individual (including the normal control and patients); reversely, other data were included as normal events (Tan et al., 2023). The advantage of this method is that it represents the continuous linear accumulation of changes caused by pathologic damage, rather than an instantaneous switch from normal to abnormal (Zhou et al., 2023). We calculated respective EBMs for (i) MCI, (ii) AD, and (iii) all patients together. We present EBMs as positional density heat maps, also known as positional variance diagrams (Fonteijn et al., 2011). The more frequent the occurrence of the events, the higher they are in the order of disease progression. We defined each participant to their maximum-likelihood numerical stage within the model (Young et al., 2014). Patients can be staged by identifying the events (subfield structural changes) within the event sequence that have already become abnormal (Eshaghi et al., 2018; Fonteijn et al., 2011; Young et al., 2014). The Bhattacharrya coefficient (BC) was used to measure the similarity for the models between MCI, AD, and all patients (Liese & Miescke, 2008; Oxtoby et al., 2021; Tan et al., 2023). Since the ordering of events depends on the data and the progression of disease, the similarity of the baseline models reflects the credibility of the model. EBM code is available at https://github.com/ucl-mig.

2.6 | Longitudinal consistency

The follow-up data were processed independently for EBM as the baseline data. We assessed the predictive capabilities of the EBM under the hypothesis that the stage increases with time, in line with our understanding of AD as a progressive disease. This was tested by estimating MCI and AD subjects' stages at 2-year follow-up and comparing to baseline.

2.7 | Correlation with memory performance

The composite episodic memory score was derived from the ADNI database (Crane et al., 2012). The score was calculated from four memory tests: memory components of MMSE, AD assessment schedule–cognition (ADAS-Cog, three versions), longitudinal Rey Auditory Verbal Learning Test (RAVLT, two versions), and logical memory task. The scores have a mean of 0 and a standard deviation (SD) of 1 (Crane et al., 2012). The score was used to verify the staging under the hypothesis that a subject with a high EBM stage will have a poor memory performance.

2.8 | Statistical analysis

Demographics and cognitive outcomes were compared between diagnostic groups using analysis of variance (ANOVA) for continuous variables and Chi-squared for categorical variables in all subjects and within diagnostic groups. Partial correlation analyses were conducted to determine the relationship between the EBM VR/AI stage and memory score in all patients and within diagnostic groups regressing out the covariates (including age, gender, and education).

3 | RESULTS

3.1 | Participants

Briefly, we included 207 subjects: 86 MCI, 53 AD and 68 NC from the ADNI-2 database who had a baseline and 2-year follow-up MRI assessments. Clinical and demographic data of study participants are presented in Table 1.

TABLE 1 Demographic and clinical characteristics of NC, MCI, and AD.

Variable	NC, $N = 68$ Mean (SD)	MCI, $N = 86$ Mean (SD)	AD, $N = 53$ Mean (SD)	p-values
Age	72.56 ± 6.01	72.98 ± 7.14	75.45 ± 8.11	.059
Education	16.35 ± 2.76^{ac}	16.01 ± 2.73	15.04 ± 2.90^{ac}	.031
Gender (M/F)	31/37	49/37	33/20	.159
MMSE	$29.06 \pm 1.29^{ab,ac}$	$27.63 \pm 1.64^{ab,bc}$	$22.79 \pm 2.48^{ac,bc}$	<.001
CDR	$0^{ab,ac}$	$.5^{ab,bc}$	$.78 \pm .27^{ac,bc}$	<.001
Memory score	$.824 \pm .472^{ab,ac}$	$.126 \pm .412^{ab,bc}$	$-.689 \pm .371^{ac,bc}$	<.001

Superscripts indicate that the pairwise groups have statistical significance using the LSD (if homogeneity of variance) or Game-Howell (if heterogeneity of variance). Chi-square test for gender distribution differences assessment.
Abbreviations: AD, Alzheimer's disease; CDR, Clinical Dementia Rating; LSD, least significant difference; MCI, mild cognitive impairment; Memory, harmonized composite memory score; MMSE, Mini-Mental State Examination, NC, normal cognition; SD, standard deviation.
[a]NC, [b]MCI, [c]AD.
[ab]Significant difference $p < .05$ between NC and MCI.
[ac]Significant difference $p < .05$ between NC and AD.
[bc]Significant difference $p < .05$ between MCI and AD.

TABLE 2 Hippocampal subfield volume-to-eHP volume (10^{-2}) of three groups at baseline.

Subfield	NC	MCI	AD	p-values
Tail	14.50 ± 1.38	14.71 ± 1.49	14.76 ± 1.57	.563
Subiculum	$12.66 \pm .57^{ab,ac}$	$12.44 \pm .73^{ab}$	$12.14 \pm .64^{ac}$	<.001
CA1	$19.11 \pm .93^{ac}$	19.29 ± 1.01^{bc}	$19.84 \pm 1.15^{ac,bc}$	<.001
HP fissure	$5.50 \pm .82^{ab,ac}$	$5.94 \pm .98^{ab,bc}$	$6.44 \pm .82^{ac,bc}$	<.001
Presubiculum	$8.46 \pm .61$	$8.38 \pm .67$	$8.20 \pm .70$	.079
Parasubiculum	$1.86 \pm .36$	$1.84 \pm .34$	$1.83 \pm .41$	.865
ML	$16.60 \pm .31^{ab,ac}$	$16.43 \pm .37^{ab}$	$16.34 \pm .39^{ac}$	<.001
GC-ML-DG	$8.67 \pm .43$	$8.77 \pm .46$	$8.82 \pm .49$	.174
CA3	$6.32 \pm .59$	$6.44 \pm .59$	$6.47 \pm .64$	.329
CA4	$7.49 \pm .37$	$7.61 \pm .40$	$7.69 \pm .45$	.025
Fimbria	$2.49 \pm .56^{ac}$	$2.30 \pm .63$	$2.10 \pm .67^{ac}$	.003
HATA	$1.84 \pm .16$	$1.89 \pm .20$	$1.83 \pm .24$	.128

Superscripts indicate that the pairwise groups have statistical significance using the LSD.
Abbreviations: AD, Alzheimer's disease; CA, cornus ammonis; GC-ML-DG, the molecular and granule cell layers of the dentate gyrus; HATA, hippocampal amygdalar transition area; HP, hippocampus; LSD, least significant difference; MCI, mild cognitive impairment; ML, the molecular layer; NC, normal control.
[a]NC, [b]MCI, [c]AD,
[ab]Significant difference $p < .05/12 = .004$ between NC and MCI.
[ac]Significant difference $p < .05/12 = .004$ between NC and AD.
[bc]Significant difference $p < .05/12 = .004$ between MCI and AD.

At baseline, education, MMSE, CDR, and memory score differed significantly between groups (education: $p = .031$, MMSE, CDR, and memory score: $p < .001$).

3.2 | Hippocampal subfield VR

At baseline, both MCI and AD patients showed larger VR in subiculum, HP fissure, and ML than NC ($p < .05$, Bonferroni corrected) controlling for age, education, and gender (Table 2). Also, AD patients had larger VR than MCI in bilateral CA1 and HP fissure (Table 2). Longitudinally, repeated measures analyses showed that MCI patients had larger VR in bilateral HP fissure and CA4 than NC ($p < .05$, Bonferroni corrected) (Table 3). AD patients had larger VR in bilateral CA1 and HP fissure, smaller VR in bilateral subiculum, and ML than NC ($p < .05$, Bonferroni corrected) (Table 3). No significance

TABLE 3 Hippocampal subfield volume -to-eHP volume (10^{-2}) of three groups at 2-year follow-up.

Subfield	NC	MCI	AD	*p*-values
Tail	14.61 ± 1.48	14.51 ± 1.59	15.07 ± 1.31	.154
Subiculum	12.68 ± .55[ac]	12.36 ± .81	12.15 ± .73[ac]	.001
CA1	19.15 ± .94[ac]	19.36 ± .98	19.82 ± 1.18[ac]	.006
HP fissure	5.61 ± .78[ab,ac]	6.15 ± 1.00[ab]	6.47 ± .84[ac]	<.001
Presubiculum	8.52 ± .55	8.37 ± .69	8.20 ± .73	.059
Parasubiculum	1.86 ± .37	1.84 ± .34	1.80 ± .33	.709
ML	16.59 ± .29[ac]	16.45 ± .37	16.32 ± .44[ac]	.002
GC-ML-DG	8.61 ± .43	8.82 ± .48	8.77 ± .52	.059
CA3	6.25 ± .59	6.52 ± .60	6.37 ± .60	.054
CA4	7.43 ± .36[ab]	7.68 ± .43[ab]	7.64 ± .44	.003
Fimbria	2.47 ± .53[ac]	2.21 ± .66	2.04 ± .67[ac]	.003
HATA	1.85 ± .17	1.89 ± .21	1.82 ± .22	.207

Superscripts indicate that the pairwise groups have statistical significance using the LSD.
Abbreviations: AD, Alzheimer's disease; CA, cornus ammonis; GC-ML-DG, the molecular and granule cell layers of the dentate gyrus; HATA, hippocampal amygdalar transition area; HP, hippocampus; MCI, mild cognitive impairment; ML, the molecular layer; NC, normal control.
[a]NC, [b]MCI, [c]AD,
[ab]Significant difference $p < .05/12 = .004$ between NC and MCI.
[ac]Significant difference $p < .05/12 = .004$ between NC and AD.
[bc]Significant difference $p < .05/12 = .004$ between MCI and AD.

in hippocampal subfield VR existed between MCI and AD groups during the 2-year follow-up period (Table 3).

3.3 | Asymmetry of hippocampal subfields

At baseline, seven subfields showed increased AI in AD patients than NC (Bonferroni corrected, $p < .004$). They included the tail, subiculum, parasubiculum, ML, GC-ML-DG, CA3, and CA4 (Table 4). Whereas compared to MCI, AD patients showed increased AI in the subiculum (Table 4). At 2-year follow-up, eight subfields showed increased AI in AD patients than NC (Bonferroni corrected, $p < .004$). They included the tail, subiculum, CA1, HP fissure, ML, GC-ML-DG, CA3, CA4, and fimbria (Table 5). Moreover, we found that AD patients showed increased AI in the subiculum, HP fissure, and CA4 compared to MCI at 2-year follow-up (Table 5). However, no difference in AI between NC and MCI existed at any time.

3.4 | Sequence of atrophy and asymmetry progression

We estimated the sequences in which these 12 hippocampal subfields become atrophic in patients with MCI and AD. In bilateral VR analysis, the first changed subfield was the HP fissure, followed by CA1, 3, 4 and GC-ML-DG, and lower-ranked subfields were subiculum, fimbria, and ML in both MCI and AD groups (Figure 1). The models show high qualitative and quantitative concordance: statistical similarity BC between MCI and AD groups was .89 ± .18, BC between MCI and all patients was.95 ± .05, and BC between AD and all patients was .91 ± .13. In left subfield VR analysis, in all patient group, atrophy of ML and fissure were estimated to start first and the parasubiculum relatively late (Figure 2). In right subfield VR analysis, in all patient group, atrophy of subiculum appeared first, followed by CA4, and finally parasubiculum, yet the following structures showed a large degree of uncertainty (Figure 2). BC between the left and right subfield was .60 ± .41. We identified marked difference between the sequences of left and right hippocampal subfields atrophy, so asymmetry pattern was further analysed.

When the EBM was used to estimate the sequence of asymemtry progression of the selected 12 hippocampal subfields, the model estimated that asymmetry progression started with the GC-ML-DG, CA4, and ML, while the late affected subfields were the parasubiculum and HP fissure (Figure 3). The models show some qualitative and quantitative concordance: statistical similarity BC between MCI and AD groups was .73 ± .24, BC between MCI and all patients was .92 ± .05, and BC between AD and all patients was .77 ± .25.

TABLE 4 Hippocampal subfield asymmetry index of three groups at baseline.

Subfield	NC	MCI	AD	*p*-values
Tail	3.66 ± 3.245[ac]	5.04 ± 3.80	6.04 ± 7.11[ac]	.022
Subiculum	2.83 ± 2.92[ac]	3.47 ± 2.56[bc]	5.50 ± 4.38[ac,bc]	<.001
CA1	3.46 ± 2.50	4.56 ± 3.38	5.01 ± 4.52	.037
HP fissure	6.91 ± 5.86	7.43 ± 5.43	9.15 ± 7.27	.119
Presubiculum	4.88 ± 3.77	5.72 ± 4.16	7.14 ± 5.97	.027
Parasubiculum	8.23 ± 6.54[ac]	8.83 ± 6.62	12.32 ± 10.32[ac]	.009
ML	2.65 ± 2.12[ac]	3.81 ± 2.91	5.01 ± 3.96[ac]	<.001
GC-ML-DG	3.62 ± 3.09[ac]	5.46 ± 4.10	6.72 ± 4.82[ac]	<.001
CA3	6.13 ± 4.27[ac]	7.79 ± 5.05	9.05 ± 6.33[ac]	.008
CA4	3.64 ± 3.27[ac]	5.22 ± 4.03	7.06 ± 4.80[ac]	<.001
Fimbria	8.41 ± 7.59	13.08 ± 13.66	14.09 ± 13.50	.016
HATA	7.44 ± 6.73	7.83 ± 6.26	8.41 ± 6.99	.723
Whole HP	2.46 ± 2.10[ac]	3.48 ± 2.62	4.88 ± 4.14[ac]	<.001

Superscripts indicate that the pairwise groups have statistical significance using the LSD.
Abbreviations: AD, Alzheimer's disease; CA, cornus ammonis; GC-ML-DG, the molecular and granule cell layers of the dentate gyrus; HATA, hippocampal amygdalar transition area HP, hippocampus; LSD, least significant difference; MCI, mild cognitive impairment; ML, the molecular layer; NC, normal cognition.
[a]NC, [b]MCI, [c]AD,
[ab]Significant difference $p < .05/13 = .004$ between NC and MCI.
[ac]Significant difference $p < .05/13 = .004$ between NC and AD.
[bc]Significant difference $p < .05/13 = .004$ between MCI and AD.

TABLE 5 Hippocampal subfield asymmetry index of three groups at 2-year follow-up.

Subfield	NC	MCI	AD	p-values
Tail	3.85 ± 3.23[ac]	4.83 ± 4.15	7.31 ± 6.24[ac]	.001
Subiculum	2.46 ± 3.77[ac]	3.73 ± 2.60[bc]	6.81 ± 5.64[ac,bc]	<.001
CA1	3.85 ± 4.56[ac]	5.06 ± 3.76	6.79 ± 6.61[ac]	.017
HP fissure	6.37 ± 4.54[ac]	7.23 ± 5.21[bc]	11.40 ± 9.27[ac,bc]	<.001
Presubiculum	5.18 ± 4.46	5.96 ± 4.22	7.43 ± 5.24	.057
Parasubiculum	8.39 ± 6.63	9.76 ± 7.16	12.01 ± 9.00	.064
ML	2.94 ± 3.88[ac]	4.21 ± 3.13	6.51 ± 6.16[ac]	.001
GC-ML-DG	3.71 ± 3.57[ac]	5.81 ± 4.49	8.54 ± 6.86[ac]	<.001
CA3	5.31 ± 4.71[ac]	7.37 ± 5.59	10.81 ± 7.55[ac]	<.001
CA4	3.43 ± 3.18[ac]	5.65 ± 4.38[bc]	8.80 ± 7.35[ac,bc]	<.001
Fimbria	7.95 ± 6.91[ac]	13.01 ± 11.02	14.60 ± 13.85[ac]	.006
HATA	7.29 ± 7.76	6.63 ± 5.81	10.54 ± 7.38	.016
Whole HP	2.67 ± 3.47[ac]	3.78 ± 2.82[bc]	6.26 ± 5.62[ac,bc]	<.001

Superscripts indicate that the pairwise groups have statistical significance using the LSD.
Abbreviations: AD, Alzheimer's disease; CA, cornus ammonis; GC-ML-DG, the molecular and granule cell layers of the dentate gyrus; HATA, hippocampal amygdalar transition area; HP, hippocampus; LSD, least significant difference; MCI, mild cognitive impairment; ML, the molecular layer; NC, normal cognition.
[a]NC, [b]MCI, [c]AD,
[ab]Significant difference $p < .05/13 = .004$ between NC and MCI.
[ac]Significant difference $p < .05/13 = .004$ between NC and AD.
[bc]Significant difference $p < .05/13 = .004$ between MCI and AD.

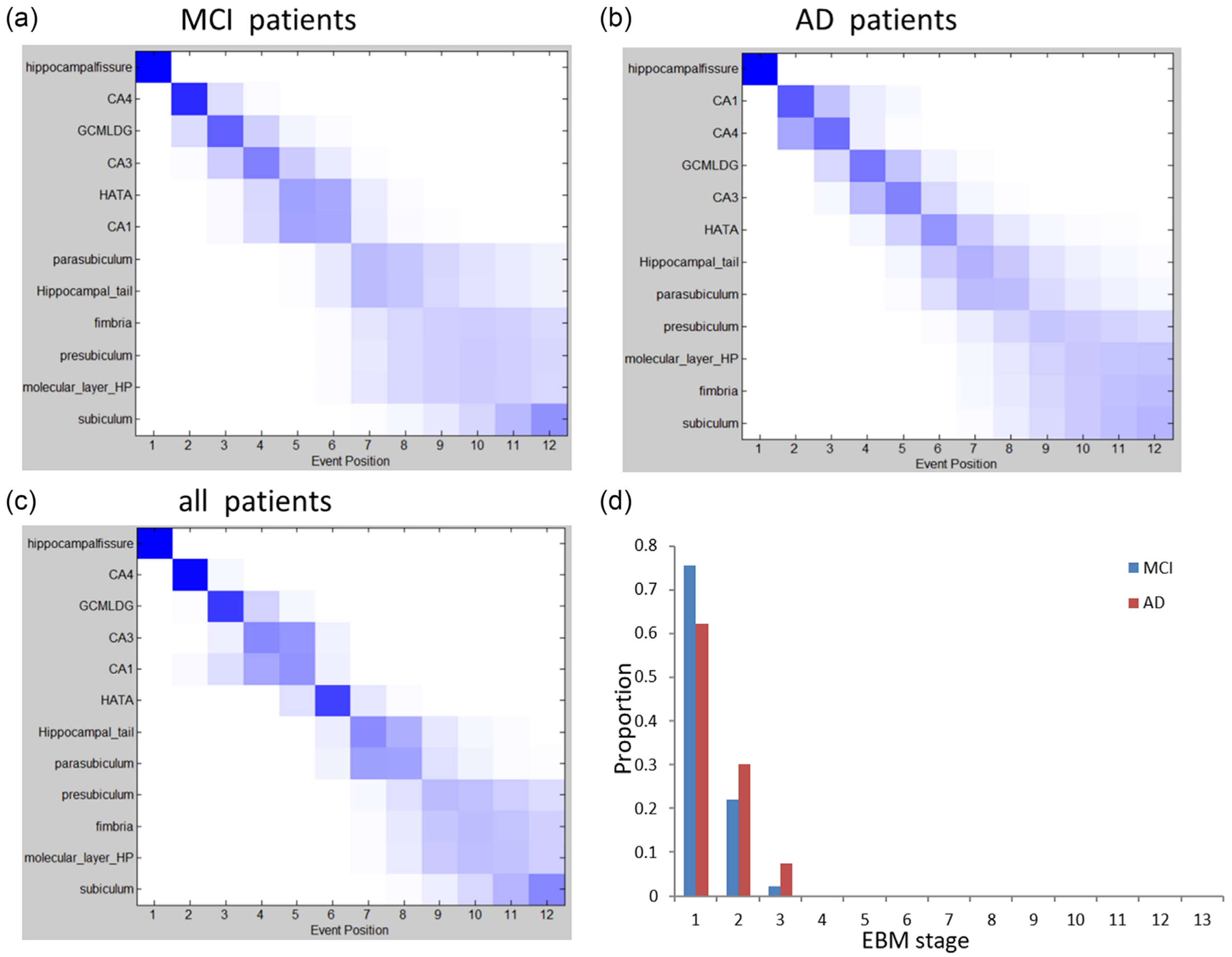

FIGURE 1 Sequences of atrophy progression and patient staging. The positional variance diagrams for (a) MCI, (b) AD and (c) merged cohort of patients, show the maximum likelihood sequences of atrophy and their associated uncertainty. In (a)–(c), the *y*-axis shows the maximum likelihood sequence of atrophy progression, and the *x*-axis shows the sequence position ranging from one to the total number of subfields. Colour intensity of the squares represents the posterior confidence in each hippocampal subfield's position in the sequence. The location of highest colour intensity means the most probable sequence of this subfield. (d) Distribution of subject EBM stages. The proportion is with respect to the total patients. AD, Alzheimer's disease; CA, cornus ammonis; EBM, event-based model; GC-ML-DG, the molecular and granule cell layers of the dentate gyrus; HATA, hippocampal amygdalar transition area; HP, hippocampus; MCI, mild cognitive impairment; ML, the molecular layer.

3.5 | Patient staging

We assigned each participant to their most likely numerical stage within the model (Fonteijn et al., 2011). Histograms of the staging results are shown in Figures 1(d) and 3(d). In VR analysis, both MCI and AD cohorts were clustered at the early stages, with the majority at stage 1. In AI analysis, the AD cohort was distributed throughout the sequence with the peak at the first event, whereas the MCI cohort was clustered at the early stages with >60% at Stage 1. This suggests that the cohort of AD cases was temporally more heterogeneous which supports the importance of accurately staging patients using objective biomarkers.

3.6 | Longitudinal consistency

The longitudinal consistency of the EBM staging system was tested using 2-year follow-up data. Figure 4(a,b) show the EBM stages at baseline versus the EBM stages at 2-year follow-up. Overall, on this metric, the EBM showed good longitudinal consistency with each subjects EBM stage generally increasing or remaining stable at 2-year follow-up: 195/207 cases (94.24%) in VR and 174/207 cases (84.17%) in AI either stayed at the same stage or progressed. In VR analysis, of the 12 MCI/AD cases that reverted in stage, nine only dropped one stage, whereas three dropped two stages (Figure 4(a)). In AI analysis, of the 33 MCI/AD cases that reverted in stage,

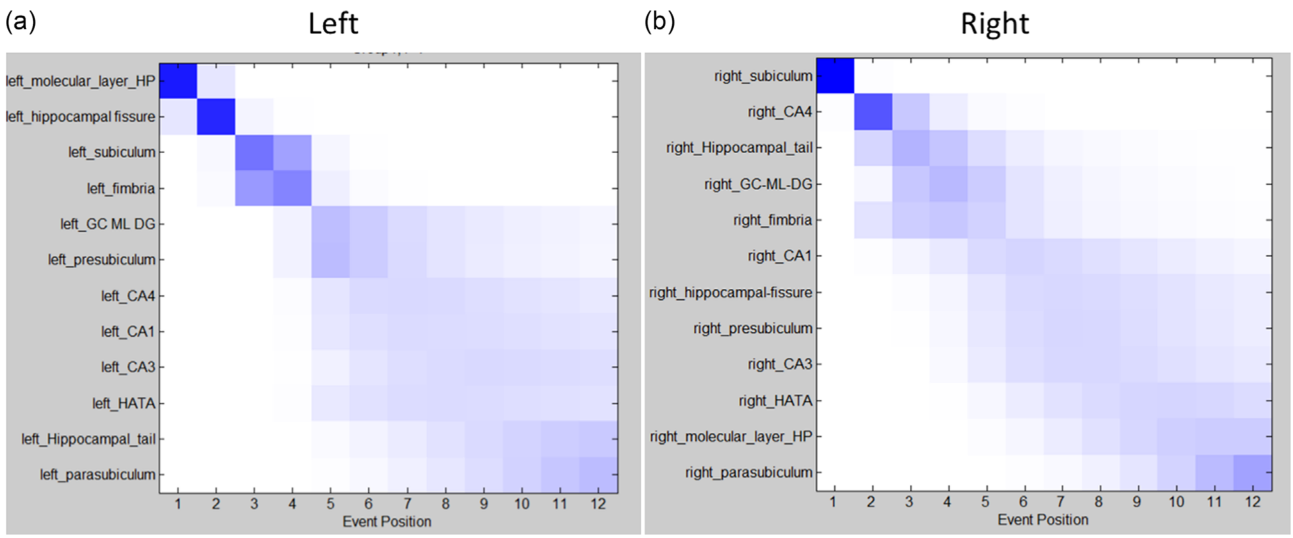

FIGURE 2 Sequences of atrophy progression in all patients. The maximum likelihood map for (a) left hippocampal subfields and (b) right hippocampal subfields. Colour intensity of the squares represents the posterior confidence in each hippocampal subfield's position in the sequence. The location of highest colour intensity means the most probable sequence of this subfield. CA, cornus ammonis; GC-ML-DG, the molecular and granule cell layers of the dentate gyrus; HATA, hippocampal amygdalar transition area; HP, hippocampus; ML, the molecular layer.

nine only dropped one stage, nine dropped two stages, eight dropped three stages, two dropped four stages, three dropped five stages, and two dropped six stages (Figure 4(b)). It confirms that the subject stages generally increase, or stay constant with time, as expected. Few of the cases drop stages. The EBM showed a good longitudinal consistency.

3.7 | Correlation with memory performance

We tested whether the EBM stages were related to memory after correcting for age, sex, and education. At baseline, the AI EBM stage was negatively correlated with memory score ($p = .019$, $r = -.201$; Figure 5) in MCI and AD patients. However, there was no association between the VR EBM stages and the memory in any clinical phenotype.

4 | DISCUSSION

We used a data-driven EBM to simulate AD disease progression. We revealed the maximum likelihood sequence in which hippocampal subfields become atrophic and asymmetric in MCI and AD patients. These sequences were consistent in key subfields: hippocampal fissure was the earliest region to become atrophic; GC-ML-DG, CA4, and ML were among the earliest regions to become asymmetric in both MCI and AD patients. Longitudinal analysis performed using 2 years of follow-up data from baseline confirms efficacy of the model. 94.24% in VR and 84.17% in AI remained in the same stage or progressed to a later stage over 2 years. The model derived AI staging correlated with memory.

The order of atrophy progression in the EBM for most regions was similar between MCI and AD. This is in agreement with AD neurodegenerative process, since MCI is either a prodromal stage (according to the 2011 NIA-AA nomenclature) or clinical Stage 3 (according to the 2018 NIA-AA framework) of AD and the pathological processes are regionally consistent between MCI and AD patients (Braak & Braak, 1990; Duyckaerts & Hauw, 1997). The earliest VR change in our model occurs in the hippocampal fissure, then spreading to other subfields. The early involvement of the fissure is well reported (Izzo et al., 2020; Murray et al., 2021; Qu et al., 2023; Worker et al., 2018). Hippocampal fissure volume was found as an early neuroimaging biomarker to assist the clinical diagnosis of MCI and AD (Izzo et al., 2020; Qu et al., 2023). Interestingly, our findings suggest the early VR of the hippocampal fissure enlargement in MCI and AD. But this did not mean the hypertrophy of the hippocampal fissure. Actually, all of the hippocampal subfields showed atrophy in the MCI and AD group (Supplementary Table S1). Given that differences in the hippocampal subfield pathology are found in AD (Braak & Braak, 1991; Fukutani et al., 2000; Lace et al., 2009; Schönheit et al., 2004), we chose to focus on

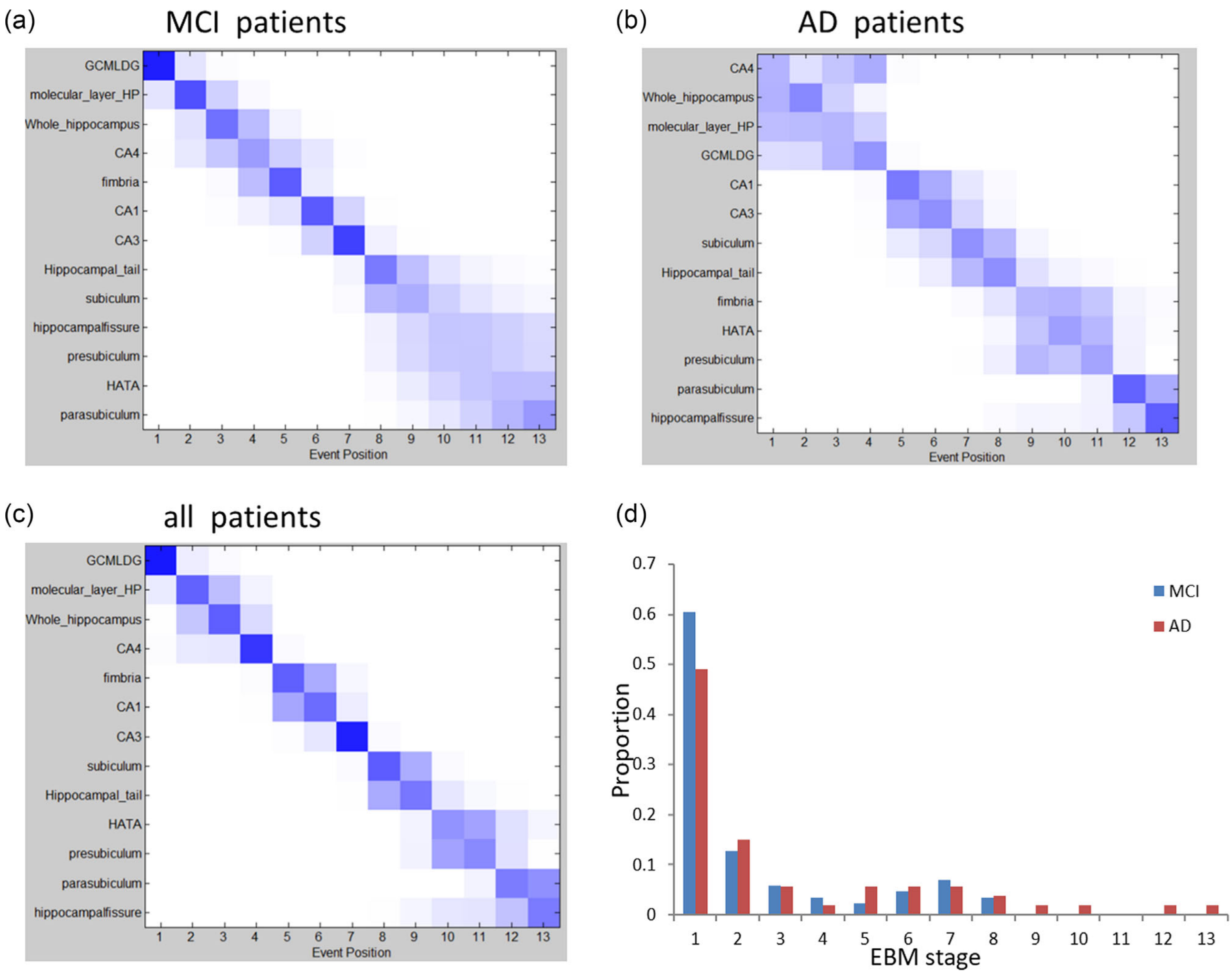

FIGURE 3 Sequences of asymmetry progression and patient staging. The positional variance diagrams for (a) MCI, (b) AD, and (c) merged cohort of patients, show the maximum likelihood sequences of atrophy and their associated uncertainty. In (a)–(c), the *y*-axis shows the maximum likelihood sequence of asymmetry progression, and the *x*-axis shows the sequence position ranging from one to the total number of subfields. Colour intensity of the squares represents the posterior confidence in each hippocampal subfield's position in the sequence. The location of highest colour intensity means the most probable sequence of this subfield. (d) Distribution of subject EBM stages. The proportion is with respect to the total patients. AD, Alzheimer's disease; CA, cornus ammonis; EBM, event-based model; GC-ML-DG, the molecular and granule cell layers of the dentate gyrus; HATA, hippocampal amygdalar transition area; HP, hippocampus; MCI, mild cognitive impairment; ML, the molecular layer.

the ratio of volumes as our target measure of interest. We also tried to build a EBM model based on the subflieds' volumes (Supplementary Figure S2). The result showed an overlap among each subfield reflects the uncertainty in the order. But we still can find the earliest atrophy in the hippocampal fissure in MCI and AD patients.

By further similarity comparison, we found that the sequence of left subfield atrophy progression was different from that of the right side in MCI and AD patients, although the fissure was impacted relatively early on both sides. Therefore, we further investigated the asymmetry analyses. AI EBM model placed GC-ML-DG, CA4, and ML before CA1 and subiculum, and overall predicted a central-to-peripheral pattern of asymmetry progression. This may support the evidence from tau deposition pattern within HP in AD (Bobinski et al., 1998; Lace et al., 2009; West et al., 2004). Lace et al. revealed a spread of tau malfunction through neuroanatomical pathways began in the inner ML (Lace et al., 2009). In line with tau pathology, according to hippocampal trisynaptic circuit, signals from the entorhinal cortex transmit to DG, then to CA1–3, finally to the subiculum (Stepan et al., 2015). This parallel pattern between atrophy asymmetry progression and pathology and neuronal connections suggests that they should be related, although this relationship is not fully elucidated. Our findings provided support for the hypothesis that disease processes may spread via tau pathology or/and neuronal connections.

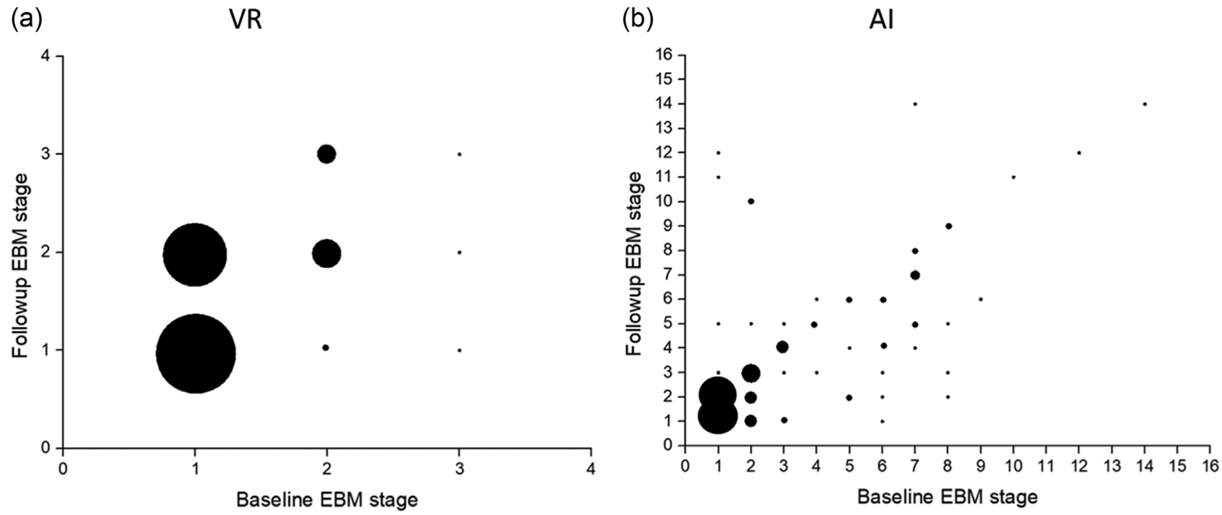

FIGURE 4 Longitudinal consistency of baseline EBM. (a) VR EBM stages, (b) AI EBM stages. Scatter plot showing predicted stage at baseline (x-axis) versus predicted stage at 2-year (y-axis) for those MCI and AD subjects with a follow-up scan (n = 207). The area of a circle is weighted by the number of subjects at each point (the bigger the circle, the more the subjects at this point). AD, Alzheimer's disease; AI, asymmetry index; EBM, event-based model; MCI, mild cognitive impairment; VR, volume ratio.

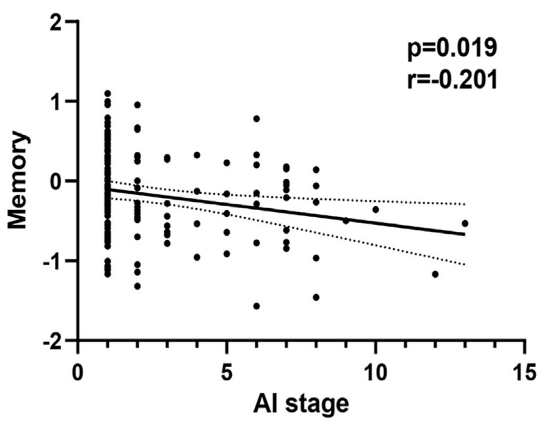

FIGURE 5 The AI EBM stage was negatively correlate with memory score in MCI and AD patients. AD, Alzheimer's disease; AI, asymmetry index; EBM, event-based model; MCI, mild cognitive impairment.

Although previous studies have found a general trend of increased degree of asymmetry of hippocampal subfields with increasing severity of diagnosis of AD (Maruszak & Thuret, 2014; Sarica et al., 2018), we know relatively little about its progression. The current study fills this gap by using MRI to examine for the first time the asymmetric progression of the hippocampal subfields implicated in AD. Analysing both volumetric atrophy and asymmetry patterns could inform the development of individualized MRI biomarkers (Alhusaini et al., 2012). Thus, it was very interesting to visualize these orderings of asymmetric hippocampal subfields' events in AD progression. These findings were validated by correlating the patient stages derived from asymmetry orderings with memory scores. The negative correlation underlies the progress of the disease and offers the potential for novel therapeutic intervention to ameliorate progression of memory impairment by interrupting anatomical progression.

A particular strength of our study is the analysis of a 2-year follow up data which supports many of our conclusions at the baseline in both cohorts. Specifically, the EBM showed quantitative agreement on the early injury of CA4 and GC-ML-DG. This is quite consistent with previous studies reporting that CA4 and GC-ML-DG regions were both sensitive (Huang et al., 2022; Liang et al., 2018). More in detail, the researchers found that atrophy of these two regions might be an early biomarker for distinguishing NC from MCI and predicting memory impairment (Huang et al., 2022; Liang et al., 2018; Novellino et al., 2018). In AD, where no effective treatment is available at the moment, selective enrolment applying CA4 and GC-ML-DG as imaging biomarkers can be applied for testing innovative treatments targeting not only AD stages but also memory deficits phenomena.

We found that memory was negatively associated with asymmetry stages in MCI and AD patients. In addition, the AI of GC-ML-DG, CA4, and ML was negatively correlated with memory scores (CA4: $p = .006$, $r = -.234$; GC-ML-DG: $p = .019$, $r = -.201$; ML: $p = .034$, $r = -.182$). While in VR analysis, no significant relationship was found between the stages and the memory in any groups. The VR of hippocampal fissure was significantly correlated with memory scores ($p < .001$, $r = -.319$). Overall, the different relationships between memory performance and hippocampal subfield morphology are reflected in different researches. For example, selected subfield (e.g. CA4, DG, subiculum) atrophy has been shown to correlate with memory performance (Carlesimo et al., 2015; O'Shea et al., 2022). In a study of AD and dementia with Lewy bodies, no association was found between hippocampal subfield volumes and memory function decline (Borda et al., 2020). Even an inverse association was observed, in which smaller volume was associated with better memory performance (Caillaud et al., 2020). This discrepancy pattern could be due to various ways of measuring memory or subject differences. We suppose that in addition to structural atrophy, asymmetry changes should be a more reliable biomarker in the study of memory decline. In line with previous studies (Toga & Thompson, 2003; Woolard & Heckers, 2012), the asymmetry of the subfield may serve as a neuroanatomical marker to predict memory.

5 | LIMITATION

This study design has several limitations. First, we only included MCI patients who were relatively stable during the 2-year follow-up. None of them progressed to AD or reversed to NC. It is suggested to assess hippocampal subfield atrophy asymmetry in future studies in other preclinical AD diseases such as amnestic MCI, semantic MCI, and subjective cognitive decline. Second, we used 3D-T1 images from ADNI-2 dataset. Although FreeSurfer has been a widely used and validated automated hippocampal subfield segmentation tool, the segmentation results of the hippocampal subfields should also be validated at higher resolution or using other automated segmented tools in the future. Third, due to the small sample sizes included in the present study, we suggest that it would be beneficial in future to assess these reliability metrics in a larger sample with three or more time points to validate our findings. Prospective data is preferred with enough follow-up time to allow for conversion of MCI patients to AD.

6 | CONCLUSION

We used data-driven event-based modeling to determine the sequence of atrophy and asymmetry progression of hippocampal subfields in MCI and AD patients. The models showed similarity in many key sub-regions between the two cohorts and good longitudinal consistency between baseline and a 2-year follow-up. The characteristic sequences fit the current understanding of AD tau pathology and neuronal connections of HP. We gained new insights into the disease stages as well as memory decline. We expect that these disease progression models will benefit patient monitoring in the future, and may help optimize novel therapeutic intervention for memory deficits.

AUTHOR CONTRIBUTIONS

Jingjing Xu: Conceptualization, data curation, formal analysis, funding acquisition, investigation, methodology, project administration, visualization, writing—original draft, writing—review and editing. **Sijia Tan:** Data curation, investigation, writing—original draft preparation, writing—review and editing. **Jiaqi Wen:** Investigation, writing—original draft preparation, writing—review and editing. **Minming Zhang:** Project administration, supervision, writing—original draft preparation, writing—review and editing. **Xiaojun Xu:** Methodology, investigation, project administration, supervision, writing—original draft preparation, writing—review and editing.

ACKNOWLEDGEMENTS

The authors would like to thank research assistant Ehsan Ghoushi. We would further like to acknowledge all participants and the many colleagues of the ADNI dataset.

CONFLICT OF INTEREST STATEMENT

The authors declare no conflicts of interest.

PEER REVIEW

The peer review history for this article is available at https://www.webofscience.com/api/gateway/wos/peer-review/10.1111/ejn.16543.

DATA AVAILABILITY STATEMENT

The datasets used and/or analysed during the current study are available from the corresponding author on reasonable request. Structural analyses were conducted using FreeSurfer's V6.0 recon-all pipeline (http://surfer.nmr.mgh.harvard.edu). EBM code is available at https://github.com/ucl-mig.

ORCID

Minming Zhang https://orcid.org/0000-0003-0145-7558
Xiaojun Xu https://orcid.org/0000-0002-0127-2812

REFERENCES

Alhusaini, S., Doherty, C. P., Palaniyappan, L., Scanlon, C., Maguire, S., Brennan, P., Delanty, N., Fitzsimons, M., & Cavalleri, G. L. (2012). Asymmetric cortical surface area and morphology changes in mesial temporal lobe epilepsy with hippocampal sclerosis. *Epilepsia*, *53*(6), 995–1003. https://doi.org/10.1111/j.1528-1167.2012.03457.x

Apostolova, L. G., Hwang, K. S., Andrawis, J. P., Green, A. E., Babakchanian, S., Morra, J. H., Cummings, J. L., Toga, A. W., Trojanowski, J. Q., Shaw, L. M., Jack, C. R. Jr., Petersen, R. C., Aisen, P. S., Jagust, W. J., Koeppe, R. A., Mathis, C. A., Weiner, M. W., Thompson, P. M., & Alzheimer's Disease Neuroimaging Initiative. (2010). 3D PIB and CSF biomarker associations with hippocampal atrophy in ADNI subjects. *Neurobiology of Aging*, *31*, 1284–1303. https://doi.org/10.1016/j.neurobiolaging.2010.05.003

Apostolova, L. G., Mosconi, L., Thompson, P. M., Green, A. E., Hwang, K. S., Ramirez, A., Mistur, R., Tsui, W. H., & de Leon, M. J. (2010). Subregional hippocampal atrophy predicts Alzheimer's dementia in the cognitively normal. *Neurobiology of Aging*, *31*, 1077–1088. https://doi.org/10.1016/j.neurobiolaging.2008.08.008

Bobinski, M., de Leon, M. J., Tarnawski, M., Wegiel, J., Reisberg, B., Miller, D. C., & Wisniewski, H. M. (1998). Neuronal and volume loss in CA1 of the hippocampal formation uniquely predicts duration and severity of Alzheimer disease. *Brain Research*, *805*(1–2), 267–269. https://doi.org/10.1016/s0006-8993(98)00759-8

Borda, M. G., Jaramillo-Jimenez, A., Tovar-Rios, D. A., Ferreira, D., Garcia-Cifuentes, E., Vik-Mo, A. O., Aarsland, V., Aarsland, D., & Oppedal, K. (2020). Hippocampal subfields and decline in activities of daily living in Alzheimer's disease and dementia with Lewy bodies. *Neurodegenerative Disease Management*, *10*(6), 357–367. https://doi.org/10.2217/nmt-2020-0039

Boutet, C., Chupin, M., Lehéricy, S., Marrakchi-Kacem, L., Epelbaum, S., Poupon, C., Wiggins, C., Vignaud, A., Hasboun, D., Defontaines, B., Hanon, O., Dubois, B., Sarazin, M., Hertz-Pannier, L., & Colliot, O. (2014). Detection of volume loss in hippocampal layers in Alzheimer's disease using 7 T MRI: A feasibility study. *Neuroimage Clinical*, *5*, 341–348. https://doi.org/10.1016/j.nicl.2014.07.011

Braak, H., & Braak, E. (1990). Alzheimer's disease: Striatal amyloid deposits and neurofibrillary changes. *Journal of Neuropathology and Experimental Neurology*, *49*(3), 215–224. PMID: 1692337. https://doi.org/10.1097/00005072-199005000-00003

Braak, H., & Braak, E. (1991). Neuropathological stageing of Alzheimer-related changes. *Acta Neuropathologica*, *82*, 239–259. https://doi.org/10.1007/BF00308809

Burwell, R. D., & Agster, K. L. (2008). Anatomy of the Hippocampus and the declarative memory system. In H. E. Eichenbaum (Ed.), *Systems and neuroscience* (pp. 47–66). Elsevier.

Caillaud, M., Hudon, C., Boller, B., Brambati, S., Duchesne, S., Lorrain, D., Gagnon, J. F., Maltezos, S., Mellah, S., Phillips, N., Consortium for the Early Identification of Alzheimer's Disease-Quebec, & Belleville, S. (2020). Evidence of a relation between hippocampal volume, white matter hyperintensities, and cognition in subjective cognitive decline and mild cognitive impairment. *The Journal of Gerontology. Series B, Psychological Sciences and Social Sciences*, *75*(7), 1382–1392. https://doi.org/10.1093/geronb/gbz120

Carlesimo, G. A., Piras, F., Orfei, M. D., Iorio, M., Caltagirone, C., & Spalletta, G. (2015). Atrophy of presubiculum and subiculum is the earliest hippocampal anatomical marker of Alzheimer's disease. *Alzheimer's & Dementia*, *1*(1), 24–32. https://doi.org/10.1016/j.dadm.2014.12.001

Clark, I. A., Monk, A. M., Hotchin, V., Pizzamiglio, G., Liefgreen, A., Callaghan, M. F., & Maguire, E. A. (2020). Does hippocampal volume explain performance differences on hippocampal-dependant tasks? *NeuroImage*, *221*, 117211. https://doi.org/10.1016/j.neuroimage.2020.117211

Crane, P. K., Carle, A., Gibbons, L. E., Insel, P., Mackin, R. S., Gross, A., Jones, R. N., Mukherjee, S., Curtis, S. M., Harvey, D., Weiner, M., Mungas, D., & Alzheimer's Disease Neuroimaging Initiative. (2012). Development and assessment of a composite score for memory in the Alzheimer's disease neuroimaging initiative (ADNI). *Brain Imaging and Behavior*, *6*, 502–516. https://doi.org/10.1007/s11682-012-9186-z

de Flores, R., La Joie, R., Landeau, B., Perrotin, A., Mézenge, F., de La Sayette, V., Eustache, F., Desgranges, B., & Chételat, G. (2015). Effects of age and Alzheimer's disease on hippocampal subfields: Comparison between manual and freesurfer volumetry. *Human Brain Mapping*, *36*, 463–474. https://doi.org/10.1002/hbm.22640

Duyckaerts, C., & Hauw, J. J. (1997). Diagnosis and staging of Alzheimer disease. *Neurobiology of Aging*, *18*(4 Suppl), S33–S42. https://doi.org/10.1016/s0197-4580(97)00067-5

Eichenbaum, H. (2004). Hippocampus: Cognitive processes and neural representations that underlie declarative memory. *Neuron*, *44*(1), 109–120. https://doi.org/10.1016/j.neuron.2004.08.028

Eshaghi, A., Marinescu, R. V., Young, A. L., Firth, N. C., Prados, F., Jorge Cardoso, M., Tur, C., De Angelis, F., Cawley, N., Brownlee, W. J., De Stefano, N., Laura Stromillo, M., Battaglini, M., Ruggieri, S., Gasperini, C., Filippi, M., Rocca, M. A., Rovira, A., Sastre-Garriga, J., … Ciccarelli, O. (2018). Progression of regional grey matter atrophy in multiple sclerosis. *Brain*, *141*(6), 1665–1677. https://doi.org/10.1093/brain/awy088

Fonteijn, H. M., Clarkson, M. J., Modat, M., Barnes, J., Lehmann, M., Ourselin, S., Fox, N. C., & Alexander, D. C. (2011). An event-based disease progression model and its application to familial Alzheimer's disease. *Information Processing in Medical Imaging*, *22*, 748–759. https://doi.org/10.1007/978-3-642-22092-0_61

Fonteijn, H. M., Modat, M., Clarkson, M. J., Barnes, J., Lehmann, M., Hobbs, N. Z., Scahill, R. I., Tabrizi, S. J., Ourselin, S., Fox, N. C., & Alexander, D. C. (2012). An event-based model for disease progression and its application in familial Alzheimer's disease and Huntington's disease. *NeuroImage*, *60*, 1880–1889. https://doi.org/10.1016/j.neuroimage.2012.01.062

Fukutani, Y., Cairns, N. J., Shiozawa, M., Sasaki, K., Sudo, S., Isaki, K., & Lantos, P. L. (2000). Neuronal loss and neurofibrillary degeneration in the hippocampal cortex in late-onset sporadic Alzheimer's disease. *Psychiatry and Clinical Neurosciences*, *54*, 523–529. https://doi.org/10.1046/j.1440-1819.2000.00747.x

Hedges, E. P., Dimitrov, M., Zahid, U., Brito Vega, B., Si, S., Dickson, H., McGuire, P., Williams, S., Barker, G. J., & Kempton, M. J. (2022). Reliability of structural MRI measurements: The effects of scan session, head tilt, inter-scan interval, acquisition sequence, FreeSurfer version and processing stream. *Neuroimage*, *246*, 118751. https://doi.org/10.1016/j.neuroimage.2021.118751

Huang, L., Chen, K., Hu, X., & Guo, Q. (2020). Differential atrophy in the hippocampal subfield volumes in four types of mild dementia. *Frontiers in Neuroscience*, *14*, 699. https://doi.org/10.3389/fnins.2020.00699

Huang, Y., Huang, L., Wang, Y., Liu, Y., Lo, C. Z., & Guo, Q. (2022). Differential associations of visual memory with hippocampal subfields in subjective cognitive decline and amnestic mild cognitive impairment. *BMC Geriatrics*, *22*(1), 153. https://doi.org/10.1186/s12877-022-02853-7

Iglesias, J. E., Augustinack, J. C., Nguyen, K., Player, C. M., Player, A., Wright, M., Roy, N., Frosch, M. P., McKee, A. C., Wald, L. L., Fischl, B., Van Leemput, K., & Initiative, A.'s. D. N. (2015). A computational atlas of the hippocampal formation using ex vivo, ultra-high resolution MRI: Application to adaptive segmentation of in vivo MRI. *NeuroImage*, *115*, 117–137. https://doi.org/10.1016/j.neuroimage.2015.04.042

Izzo, J., Andreassen, O. A., Westlye, L. T., & van der Meer, D. (2020). The association between hippocampal subfield volumes in mild cognitive impairment and conversion to Alzheimer's disease. *Brain Research*, *1728*, 146591. https://doi.org/10.1016/j.brainres.2019.146591

Jahanshahi, A. R., Naghdi Sadeh, R., & Khezerloo, D. (2023). Atrophy asymmetry in hippocampal subfields in patients with Alzheimer's disease and mild cognitive impairment. *Experimental Brain Research*, *241*(2), 495–504. https://doi.org/10.1007/s00221-022-06543-z

Lace, G., Savva, G. M., Forster, G., de Silva, R., Brayne, C., Matthews, F. E., Barclay, J. J., Dakin, L., Ince, P. G., Wharton, S. B., & MRC-CFAS. (2009). Hippocampal tau pathology is related to neuroanatomical connections: An ageing population-based study. *Brain*, *132*, 1324–1334. https://doi.org/10.1093/brain/awp059

Liang, X., Yin, Z., Liu, R., Zhao, H., Wu, S., Lu, J., Qing, Z., Wei, Y., Yang, Q., Zhu, B., Xu, Y., & Zhang, B. (2018). The role of MRI biomarkers and their interactions with cognitive status and APOE ε4 in nondemented elderly subjects. *Neurodegenerative Diseases*, *18*(5–6), 270–280. https://doi.org/10.1159/000495754

Liese, F., & Miescke, K. J. (2008). *Statistical decision theory: Estimation, testing, and selection*. Springer New York.

Liu, H., Zhang, L., Xi, Q., Zhao, X., Wang, F., Wang, X., Men, W., & Lin, Q. (2018). Changes in brain lateralization in patients with mild cognitive impairment and Alzheimer's disease: A resting-state functional magnetic resonance study from Alzheimer's disease neuroimaging initiative. *Frontiers in Neurology*, *9*, 3. https://doi.org/10.3389/fneur.2018.00003

Maruszak, A., & Thuret, S. (2014). Why looking at the whole hippocampus is not enough-a critical role for anteroposterior axis, subfield and activation analyses to enhance predictive value of hippocampal changes for Alzheimer's disease diagnosis. *Frontiers in Cell Neuroscience*, *8*, 95. https://doi.org/10.3389/fncel.2014.00095

Mueller, S. G., & Weiner, M. W. (2009). Selective effect of age, Apoε4, and Alzheimer's disease on hippocampal subfields. *Hippocampus*, *19*, 558–564. https://doi.org/10.1002/hipo.20614

Murray, A. N., Chandler, H. L., & Lancaster, T. M. (2021). Multimodal hippocampal and amygdala subfield volumetry in polygenic risk for Alzheimer's disease. *Neurobiology of Aging*, *98*, 33–41. https://doi.org/10.1016/j.neurobiolaging.2020.08.022

Novellino, F., Vasta, R., Sarica, A., Chiriaco, C., Salsone, M., Morelli, M., Arabia, G., Saccà, V., Nicoletti, G., & Quattrone, A. (2018). Relationship between hippocampal subfields and category cued recall in AD and PDD: A multimodal MRI study. *Neuroscience*, *371*, 506–517. https://doi.org/10.1016/j.neuroscience.2017.12.028

O'Mara, S. M., & Aggleton, J. P. (2019). Space and memory (far) beyond the hippocampus: Many subcortical structures also support cognitive mapping and mnemonic processing. *Frontiers in Neural Circuits*, *13*, 52. https://doi.org/10.3389/fncir.2019.00052

O'Shea, D. M., de Wit, L., Tanner, J., Mejia Kurasz, A., Amofa, P., Perez Lao, A., Levy, S. A., Chandler, M., & Smith, G. (2022). Hippocampal subfields in mild cognitive impairment: Associations with objective and informant-report of memory function. *Archives of Clinical Neuropsychology*, *37*(7), 1502–1514. https://doi.org/10.1093/arclin/acac018

Oxtoby, N. P., Leyland, L. A., Aksman, L. M., Thomas, G. E. C., Bunting, E. L., Wijeratne, P. A., Young, A. L., Zarkali, A., Tan, M. M. X., Bremner, F. D., Keane, P. A., Morris, H. R., Schrag, A. E., Alexander, D. C., & Weil, R. S. (2021). Sequence of clinical and neurodegeneration events in Parkinson's disease progression. *Brain*, *144*(3), 975–988. https://doi.org/10.1093/brain/awaa461

Parker, T. D., Slattery, C. F., Yong, K. X., Nicholas, J. M., Paterson, R. W., Foulkes, A. J. M., Malone, I. B., Thomas, D. L., Cash, D. M., Crutch, S. J., Fox, N. C., & Schott, J. M. (2019). Differences in hippocampal subfield volume are seen in phenotypic variants of early onset Alzheimer's disease. *NeuroImage Clinical*, *21*, 101632. https://doi.org/10.1016/j.nicl.2018.101632

Petersen, R. C., Aisen, P. S., Beckett, L. A., Donohue, M. C., Gamst, A. C., Harvey, D. J., Jack, C. R. Jr., Jagust, W. J., Shaw, L. M., Toga, A. W., Trojanowski, J. Q., & Weiner, M. W. (2010). Alzheimer's disease neuroimaging initiative (ADNI): Clinical characterization. *Neurology*, *74*, 201–209. https://doi.org/10.1212/WNL.0b013e3181cb3e25

Pluta, J., Yushkevich, P., Das, S., & Wolk, D. (2012). In vivo analysis of hippocampal subfield atrophy in mild cognitive impairment via semi-automatic segmentation of T2-weighted MRI. *Journal of Alzheimer's Disease*, *31*, 85–99. https://doi.org/10.3233/JAD-2012-111931

Punzi, M., Sestieri, C., Picerni, E., Chiarelli, A. M., Padulo, C., Delli Pizzi, A., Tullo, M. G., Tosoni, A., Granzotto, A., Della Penna, S., Onofrj, M., Ferretti, A., Delli Pizzi, S., Sensi, S. L., & Alzheimer's Disease Neuroimaging Initiative. (2024). Atrophy of hippocampal subfields and amygdala nuclei in subjects with mild cognitive impairment progressing to Alzheimer's disease. *Heliyon*, *10*(6), e27429. https://doi.org/10.1016/j.heliyon.2024.e27429

Qu, H., Ge, H., Wang, L., Wang, W., & Hu, C. (2023). Volume changes of hippocampal and amygdala subfields in patients with mild cognitive impairment and Alzheimer's disease. *Acta Neurologica Belgica*, *123*(4), 1381–1393. https://doi.org/10.1007/s13760-023-02235-9

Roe, J. M., Vidal-Piñeiro, D., Sørensen, Ø., Brandmaier, A. M., Düzel, S., Gonzalez, H. A., Kievit, R. A., Knights, E., Kühn, S., Lindenberger, U., Mowinckel, A. M., Nyberg, L., Park, D. C., Pudas, S., Rundle, M. M., Walhovd, K. B., Fjell, A. M., Westerhausen, R., & Australian Imaging Biomarkers and Lifestyle Flagship Study of Ageing. (2021). Asymmetric thinning of the cerebral cortex across the adult lifespan is accelerated in Alzheimer's disease. *Nature Communications*, *12*, 721. https://doi.org/10.1038/s41467-021-21057-y

Sarica, A., Vasta, R., Novellino, F., Vaccaro, M. G., Cerasa, A., Quattrone, A., & Alzheimer's Disease Neuroimaging Initiative. (2018). MRI asymmetry index of hippocampal subfields increases through the continuum from the mild cognitive impairment to the Alzheimer's disease. *Frontiers in Neuroscience*, *12*, 576. https://doi.org/10.3389/fnins.2018.00576

Schönheit, B., Zarski, R., & Ohm, T. G. (2004). Spatial and temporal relationships between plaques and tangles in Alzheimer-pathology. *Neurobiology of Aging*, *25*, 697–711. https://doi.org/10.1016/j.neurobiolaging.2003.09.009

Stepan, J., Dine, J., & Eder, M. (2015). Functional optical probing of the hippocampal trisynaptic circuit in vitro: Network dynamics, filter properties, and polysynaptic induction of CA1 LTP. *Frontiers in Neuroscience*, *9*, 160. https://doi.org/10.3389/fnins.2015.00160

Tan, S., Zhou, C., Wen, J., Duanmu, X., Guo, T., Wu, H., Wu, J., Cao, Z., Liu, X., Chen, J., Wu, C., Qin, J., Xu, J., Gu, L., Yan, Y., Zhang, B., Zhang, M., Guan, X., & Xu, X. (2023). Presence but not the timing of onset of REM sleep behavior disorder distinguishes evolution patterns in Parkinson's disease. *Neurobiology of Disease*, *180*, 106084. https://doi.org/10.1016/j.nbd.2023.106084

Tang, X., Holland, D., Dale, A. M., Younes, L., Miller, M. I., & Initiative, A.'s. D. N. (2015). The diffeomorphometry of regional shape change rates and its relevance to cognitive deterioration in mild cognitive impairment and Alzheimer's disease. *Human Brain Mapping*, *36*, 2093–2117. https://doi.org/10.1002/hbm.22758

Toga, A. W., & Thompson, P. M. (2003). Mapping brain asymmetry. *Nature Reviews. Neuroscience*, *4*, 37–48. https://doi.org/10.1038/nrn1009

Tognin, S., van Hell, H. H., Merritt, K., Winter-van Rossum, I., Bossong, M. G., Kempton, M. J., Modinos, G., Fusar-Poli, P., Mechelli, A., Dazzan, P., Maat, A., de Haan, L., Crespo-Facorro, B., Glenthøj, B., Lawrie, S. M., McDonald, C., Gruber, O., van Amelsvoort, T., Arango, C., … PSYSCAN Consortium. (2020). Towards precision medicine in psychosis: Benefits and challenges of multimodal multicenter studies-PSYSCAN: Translating neuroimaging findings from research into clinical practice. *Schizophrenia Bulletin*, *46*(2), 432–441. https://doi.org/10.1093/schbul/sbz067

Wechsler, D. (1987). *The Wechsler memory scale-revised*. Psychological Corporation.

Weise, C. M., Chen, K., Chen, Y., Kuang, X., Savage, C. R., Reiman, E. M., & Alzheimer's Disease Neuroimaging Initiative. (2018). Left lateralized cerebral glucose metabolism declines in amyloid-β positive persons with mild cognitive impairment. *NeuroImage Clinical*, *20*, 286–296. https://doi.org/10.1016/j.nicl.2018.07.016

West, M. J., Kawas, C. H., Stewart, W. F., Rudow, G. L., & Troncoso, J. C. (2004). Hippocampal neurons in pre-clinical Alzheimer's disease. *Neurobiology of Aging*, *25*(9), 1205–1212. https://doi.org/10.1016/j.neurobiolaging.2003.12.005

Wisse, L. E., Biessels, G. J., Heringa, S. M., Kuijf, H. J., Koek, D. H., Luijten, P. R., Geerlings, M. I., & Utrecht Vascular Cognitive Impairment (VCI) Study Group. (2014). Hippocampal subfield volumes at 7T in early Alzheimer's disease and normal aging. *Neurobiology of Aging*, *35*, 2039–2045. https://doi.org/10.1016/j.neurobiolaging.2014.02.021

Woolard, A. A., & Heckers, S. (2012). Anatomical and functional correlates of human hippocampal volume asymmetry. *Psychiatry Research*, *201*, 48–53. https://doi.org/10.1016/j.pscychresns.2011.07.016

Worker, A., Dima, D., Combes, A., Crum, W. R., Streffer, J., Einstein, S., Mehta, M. A., Barker, G. J., Williams, S. C. R., & O'daly, O. (2018). Test-retest reliability and longitudinal analysis of automated hippocampal subregion volumes in healthy ageing and Alzheimer's disease populations. *Human Brain Mapping*, *39*(4), 1743–1754. https://doi.org/10.1002/hbm.23948

Wu, X., Wu, Y., Geng, Z., Zhou, S., Wei, L., Ji, G. J., Tian, Y., & Wang, K. (2020). Asymmetric differences in the gray matter volume and functional connections of the amygdala are associated with clinical manifestations of Alzheimer's disease. *Frontiers in Neuroscience*, *14*, 602. https://doi.org/10.3389/fnins.2020.00602

Xu, J., Guan, X., Wen, J., Zhang, M., Xu, X., & Alzheimer's Disease Neuroimaging Initiative. (2022). Polygenic hazard score modified the relationship between hippocampal subfield atrophy and episodic memory in older adults. *Frontiers in Aging Neuroscience*, *14*, 943702. https://doi.org/10.3389/fnagi.2022.943702

Yassa, M. A., Stark, S. M., Bakker, A., Albert, M. S., Gallagher, M., & Stark, C. E. L. (2010). High resolution structural and functional MRI of hippocampal CA3 and dentate gyrus in patients with amnestic mild cognitive impairment. *NeuroImage*, *51*, 1242–1252. https://doi.org/10.1016/j.neuroimage.2010.03.040

Young, A. L., Oxtoby, N. P., Daga, P., Cash, D. M., Fox, N. C., Ourselin, S., Schott, J. M., Alexander, D. C., & Alzheimer's Disease Neuroimaging Initiative. (2014). A data-driven model of biomarker changes in sporadic Alzheimer's disease. *Brain: a Journal of Neurology*, *137*, 2564–2577. https://doi.org/10.1093/brain/awu176

Zeng, Q., Li, K., Luo, X., Wang, S., Xu, X., Li, Z., Zhang, T., Liu, X., Fu, Y., Xu, X., Wang, C., Wang, T., Zhou, J., Liu, Z., Chen, Y., Huang, P., Zhang, M., & The Alzheimer's Disease Neuroimaging Initiative. (2021). Distinct atrophy pattern of hippocampal subfields in patients with progressive and stable mild cognitive impairment: A longitudinal MRI study. *Journal of Alzheimer's Disease*, *79*, 237–247. https://doi.org/10.3233/JAD-200775

Zhao, W., Wang, X., Yin, C., He, M., Li, S., & Han, Y. (2019). Trajectories of the hippocampal subfields atrophy in the Alzheimer's disease: A structural imaging study. *Frontiers in Neuroinformatics*, *13*, 13. https://doi.org/10.3389/fninf.2019.00013

Zheng, F., Cui, D., Zhang, L., Zhang, S., Zhao, Y., Liu, X., Liu, C., Li, Z., Zhang, D., Shi, L., Liu, Z., Hou, K., Lu, W., Yin, T., & Qiu, J. (2018). The volume of hippocampal subfields in relation to decline of memory recall across the adult lifespan. *Frontiers in Aging Neuroscience*, *10*, 320. https://doi.org/10.3389/fnagi.2018.00320

Zhou, C., Wang, L., Cheng, W., Lv, J., Guan, X., Guo, T., Wu, J., Zhang, W., Gao, T., Liu, X., Bai, X., Wu, H., Cao, Z., Gu, L., Chen, J., Wen, J., Huang, P., Xu, X., Zhang, B., … Zhang, M. (2023). Two distinct trajectories of clinical and neurodegeneration events in Parkinson's disease. *Npj Parkinson's Disease*, *9*(1), 111. https://doi.org/10.1038/s41531-023-00556-3

SUPPORTING INFORMATION

Additional supporting information can be found online in the Supporting Information section at the end of this article.

How to cite this article: Xu, J., Tan, S., Wen, J., Zhang, M., For the Alzheimer's Disease Neuroimaging Initiative, & Xu, X. (2024). Progression of hippocampal subfield atrophy and asymmetry in Alzheimer's disease. *European Journal of Neuroscience*, *60*(8), 6091–6106. https://doi.org/10.1111/ejn.16543